



## OTDR fiber-optical chemical sensor system for detection and location of hydrocarbon leakage

J. Buerck\*, S. Roth, K. Kraemer, H. Mathieu

*Forschungszentrum Karlsruhe, Institut für Instrumentelle Analytik—IFIA,  
P.O. Box 3640, D-76021 Karlsruhe, Germany*

---

### Abstract

A distributed sensing system for apolar hydrocarbons is presented which is built from a polymer-clad silica fiber adapted to an optical time domain reflectometer (OTDR) set-up. OTDR measurements allow locating and detecting chemicals by measuring the time delay between short light pulses entering the fiber and discrete changes in the backscatter signals that are caused by local extraction of hydrocarbons into the fiber cladding. The light guiding properties of the fiber are affected by interaction of the extracted chemicals with the evanescent wave light field extending into the fiber cladding.

Distributed sensing of pure liquid hydrocarbons (HC) and aqueous HC solutions with a commercially available mini-OTDR adapted to sensing fibers of up to 1 km length could be demonstrated. A pulsed laser diode emitting at the 850 nm telecommunication wavelength was applied in the mini-OTDR to locate the HCs by analyzing the step drop (light loss) in the backscatter signal, which is induced by local refractive index (RI) increase in the silicone cladding due to the extracted HC. The prototype instrument can be applied for monitoring hydrocarbon leakage in large technical installations, such as tanks, chemical pipelines or chemical waste disposal containments.

© 2003 Elsevier B.V. All rights reserved.

*Keywords:* Optical time domain reflectometer; Polymer-clad silica; Photodetector

---

### 1. Introduction

Leaks in the bottom composite liner of landfill or chemical waste disposal containments may lead to the penetration of contaminated leachate through the barrier and transport of toxic substances into the surrounding soil and groundwater. Therefore, continuous surveillance of landfill liners and the identification of leaks are essential parts of waste management. For other large technical installations, such as chemical production plants, tank farms, or

---

\* Corresponding author. Tel.: +49-7247-822690; fax: +49-7247-824618.

*E-mail address:* jochen.buerck@ifia.fzk.de (J. Buerck).

pipelines extensive leakage monitoring is even more imperative, because fast detection and localization of a leak is required to prevent the release of huge amounts of hazardous chemicals and new contamination of the environment. However, fast identification of a leak position in a chemical waste disposal site may be difficult, e.g., if the site is lined with an underground geomembrane most leaks are point sources, not widespread. Due to the large spatial extension of such technical facilities, comprehensive and distributed monitoring techniques are necessary. In this context, distributed fiber-optic chemical sensing cables in combination with the interrogation method of optical time domain reflectometry (OTDR) could be an interesting alternative to conventional leakage control systems. Due to the fact, that a few hundred meters in length of such cables can be buried under the liner or under a big tank, e.g., in a grid-type scheme, they would fulfill the demand for distributed sensing. OTDR is a well established technique for characterization of fiber-optic networks or for the distributed sensing of physical parameters (strain, temperature, displacement) that detects information from every point along the sensing fiber by measuring from one end of the fiber [1,2]. Short light pulses are coupled into a quartz glass waveguide. While the light is transported through the fiber by total reflection, a part of it is scattered and guided back to the front end. The backscattered light signals are focused onto a fast photodetector, and the whole process is recorded in the time domain, e.g., by a digitizing oscilloscope or other fast electronic signal processing units. The localization of defects in the fiber (break or sharp bend) is achieved by determining the time delay between the excitation light pulse and a specific change in the OTDR backscatter signal related to this defect. From the time delay and the light velocity in the fiber, the position of the defect can be determined. Due to the evanescent wave tail of the light conducted in the fiber it is also possible to detect changes in the backscatter signal caused by defects in the fiber cladding. If fibers are used that have a cladding, which is permeable for chemical substances, e.g., a polymer coating, the light guiding properties of the fiber and the backscatter signal can be affected by optical effects induced in this cladding due to a penetrating chemical. Thus, it is possible to detect the presence and spatial distribution of analyte molecules along the active length of the fiber. Such a distributed chemical sensor, i.e. an optical fiber that is chemically sensitive over its entire length, will improve the performance of existing fiber-optic single-point sensors in many areas of application, because it can be spread over a larger area to be monitored and it allows getting information from multiple points in this area [3]. Especially, the visible and near-infrared (NIR) spectral range are predestined for distributed sensing because polymer-coated quartz glass fibers with relatively high light transmission can be used and systems extending over a domain from some ten meters to kilometers can be built up.

Up to now a number of papers on distributed chemical sensing with optical fibers have been published. Sensors for the distributed measurement of the pH value described in the literature utilize the absorption or fluorescence of dyes immobilized in discrete fiber sections in a cellulose acetate or a sol–gel cladding. They react upon changes in the absorption/fluorescence backscatter signal caused by changes in the pH value of the surrounding medium [4,5]. Connected to an OTDR setup these fibers provide quasi-distributed measurements but in principle they can be extended to totally distributed sensors by using completely sol–gel clad fibers. Distributed evanescent wave sensing has also been proposed for measuring oxygen concentrations along a silicone-clad fiber with an immobilized fluorescent dye by Potyrailo and Hieftje [6]. A multi-point-distributed humidity sensing system has

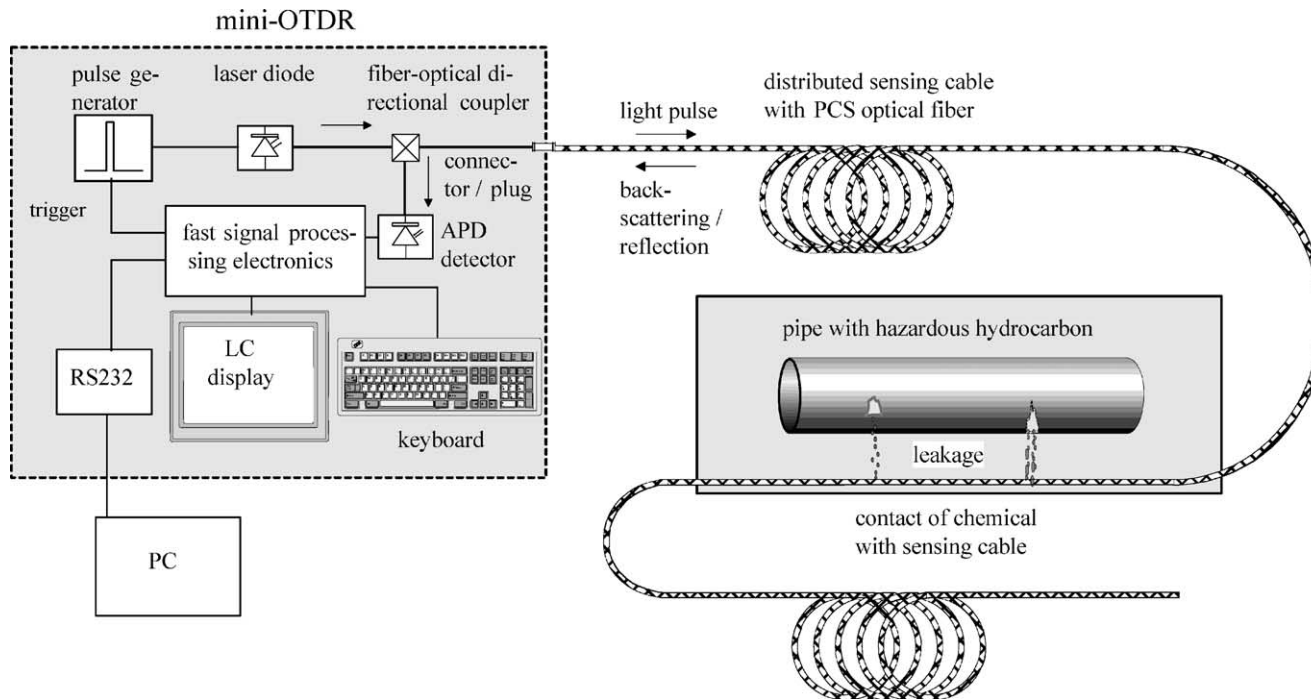


Fig. 1. Schematic view of instrumental set-up for distributed fiber-optical sensing of hydrocarbons based on optical time domain reflectometry.

been reported which is based on changes in absorption of cobalt chloride in the presence of water [7]. To build up a distributed sensor system the indicator was immobilized in a gelatin film that formed the cladding of a multimode optical fiber which was coupled to a two-wavelength OTDR setup to provide intensity referencing. Michie et al. [8,9] have demonstrated a distributed sensor system for the detection of water. The sensing fiber consists of a core, which is clad with a hydrogel and afterwards wound with a nylon string. The hydrogel swells in the presence of water, which causes microbendings in the fiber core due to the spiral nylon winding. This will lead to a partial loss of the guided light at the fiber section affected by humidity, which can be detected and located by an OTDR system.

The approach made at our institute to develop totally distributed sensor systems for hydrocarbon (HC) species is shown schematically in Fig. 1. A commercially available polymer-clad silica (PCS) fiber that is coated with a silicone polymer cladding over its entire length is adapted to a suitable OTDR instrumental set-up. The silicone polymer cladding is intrinsically sensitive to apolar hydrocarbons and recently we have presented a fiber-optical sensor for single-point measurements, where such a fiber is used for the determination of aromatic hydrocarbons in groundwater using NIR absorption spectroscopy [10]. The chemicals diffuse into the polymer cladding and are measured directly in the cladding by evanescent wave absorption interaction. Basic investigations into OTDR evanescent wave sensing with this PCS fiber revealed that different optical effects caused by HC molecules penetrating into the cladding can be used to design a distributed sensing system. Changes in the backscatter signal can either be induced by a local change of the refractive index (RI), or by varying the absorption and fluorescence properties in the fiber cladding due to the extracted HC. The different effects lead to distinct patterns in the OTDR response function, which clearly can be separated, from each other and from signals originating from mechanical defects in the fiber [11,12]. In this way hydrocarbons can be detected and located directly by OTDR measurements and additional information can be deduced because signal intensities are quantitatively correlated with the hydrocarbon concentration and the interaction length of the sensing fiber with the analyte.

In this paper we present a prototype sensor system based on a commercially available mini-OTDR which can be used for distributed sensing of HCs and aqueous HC solutions. The instrument has been adapted to PCS sensing fibers of up to nearly 1 km length. Here, laser emission at the 850 nm telecommunication wavelength was applied to locate the HCs by analyzing step drop signals (light loss) in the OTDR backscatter trace, which are caused by local increase in RI induced by analyte enrichment in the silicone cladding.

## 2. OTDR-evanescent wave sensing

### 2.1. Distributed sensing: spatial resolution by time resolved detection

The technique of optical time domain reflectometry was first demonstrated by Barnoski and Jensen [1]. OTDR typically involves launching light pulses with 10–1000 ns pulse widths into the input end of an optical fiber and measuring the return signal produced by these test pulses at the same end of the fiber. As a test pulse travels down the fiber, Rayleigh

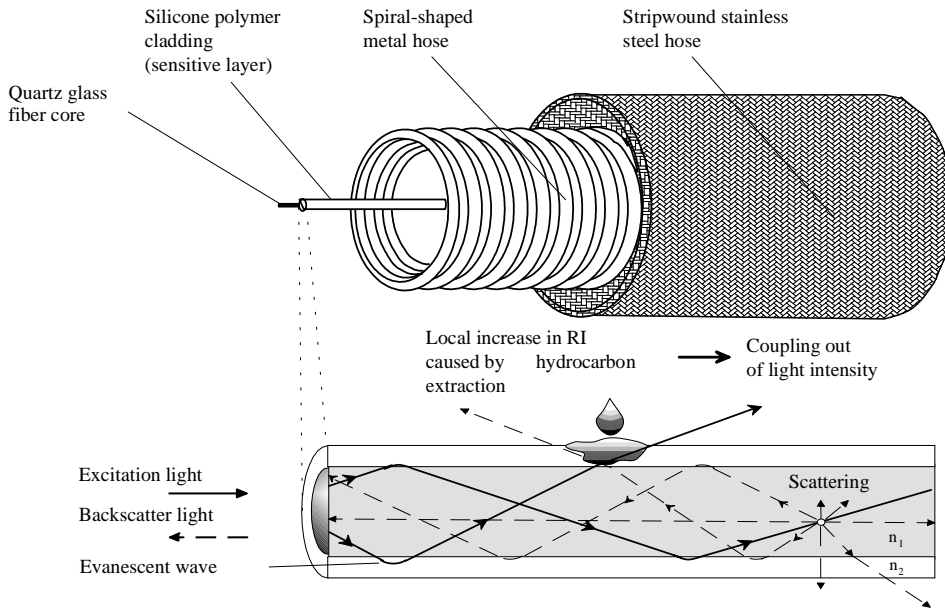


Fig. 2. Structural elements of the distributed sensing cable and illustration of evanescent wave measuring principle.

scattering and the intrinsic absorption of the fiber leads to an exponentially decreasing amplitude of the pulse. As illustrated in Fig. 2, some of this scattered light reaches the input end of the fiber to produce the measured return signal. Distinct structures in the pulse return function, which represents the magnitude of the energy incident on the detector as a function of time, allow the position of anomalous sections of an optical fiber (defect) to be determined. Such defects due to local imperfections in the fiber core/cladding manifest themselves as step drop, changes in slope or discrete reflections in the return function. The power received at the input end of the fiber from a position along the fiber  $P(x)$  has been given by Rogers [2]:

$$P(x) = \frac{1}{2} vsfc \Delta t P(0)e^{-2\delta x} \tag{1}$$

where  $v$  is the velocity of the light pulse within a quartz glass fiber =  $2.06 \times 10^8$  m/s,  $s$  the light-scattering coefficient

$$f = \frac{3}{8} \frac{n_1^2 - n_2^2}{n_1^2}$$

and  $f$  the fraction of scattered light which is recaptured by the fiber and travels back towards the input end [13],  $n_1$  the refractive index of fiber core,  $n_2$  the refractive index of fiber cladding,  $c$  the coupling efficiency of optics,  $P(0)$  the optical output power of the laser,  $\Delta t$  the pulse width of laser,  $\delta$  the total fiber attenuation caused by scattering and absorption effects in the fiber,  $x$  the position along the fiber.

Time-resolved detection following pulsed excitation can be used to probe a distributed fiber-optic sensor and locate the position of interaction with an analyte along the fiber. By evaluating the time delay  $\tau_d$  between the light pulse entering the fiber and the response signal of a discrete fiber region contacted with the analyte the spatial position of the analyte can be determined. The distance  $x$  from the fiber front to the analyte position is given by [5]

$$x = \frac{v}{2n_1} \tau_d \quad (2)$$

For a fiber that is uniformly clad over its entire length with a silicone polymer coating that enriches HC compounds, this provides a simple manner for distinguishing between response signals from different fiber zones that contact the HC analyte.

Optical modes in a step-index fiber are characterized by discrete values of the ray angles  $\theta$  ( $\theta$  is the angle of the ray with respect to the fiber axis). Each fiber mode has two modal parameters  $U$  and  $W$  given by [14]

$$U = r(n_1^2 k^2 - \beta^2)^{1/2} \quad (3)$$

$$W = r(\beta^2 - n_2^2 k^2)^{1/2} \quad (4)$$

where  $k = 2\pi/\lambda$  is the free space wavenumber ( $\lambda$  the wavelength of light),  $\beta$  the propagation constant of the mode ( $=n_1 k \cos \theta$ ), and  $r$  the fiber core radius.  $U$  and  $W$  are related to the normalized frequency  $V$  of the fiber by

$$V^2 = U^2 + W^2 \quad (5)$$

The  $V$  number is a measure for the number of modes supported by the fiber and is given by

$$V = \frac{2\pi r \sqrt{n_1^2 - n_2^2}}{\lambda} \quad (6)$$

Light guided by the core of an optical fiber will have an evanescent wave associated with it. The evanescent wave penetrates into the medium surrounding the fiber core (usually the cladding) and can interact with the material of this medium. Therefore, it is possible to obtain spectroscopic information about the cladding by observing the light guided in the core. The  $1/e$  penetration depth  $d$  of the evanescent wave in the cladding can be approximated by

$$d = \frac{r}{W} \quad (7)$$

and the transmittance  $T$  of the mode is given by [15]

$$T = \exp(-\gamma z) \quad (8)$$

where  $z$  is the length of the fiber that contacts the absorber and the evanescent wave attenuation coefficient  $\gamma$

$$\gamma = \frac{\alpha n_2 U^2}{r n_1 V W} \quad (9)$$

where  $\alpha$  is the bulk attenuation coefficient of the compound causing the evanescent wave attenuation. From Eq. (9) it can be seen that  $\gamma$  is inversely proportional to the  $V$  number, so that evanescent attenuation is stronger for few mode fibers. From Eq. (4) it can be deduced that  $W \rightarrow 0$  for highest order modes and thus  $\gamma \rightarrow \infty$ .

These theoretical equations show that the light guiding characteristics of a fiber can be affected by chemicals in the cladding in different ways. First, if a chemical extracted into the cladding increases the cladding refractive index  $n_2$ , then higher order modes will be stripped, leading to a light loss at the position of enrichment. Second, there may be a change in the bulk attenuation coefficient of the influenced fiber section arising, e.g., from light absorbing evanescent wave interactions with the extracted chemical.

### 3. Experimental

#### 3.1. Sensing fiber

A commercially available low-hydroxyl silica core fiber with a poly(dimethylsiloxane) cladding and a nylon buffer was used as the basic element of the distributed sensors. The RI of the silica core and the cladding material is 1.456 and 1.436 (at the wavelength of 633 nm), respectively, resulting in a numerical aperture of  $NA = 0.24$ . The fiber has a 100  $\mu\text{m}$  o.d. core and a 200  $\mu\text{m}$  o.d. cladding. To turn this PCS fiber into a truly distributed sensing fiber for apolar HCs, the outer nylon buffer with a thickness of 35  $\mu\text{m}$  was removed chemically over the full length of the fiber. It was dissolved by boiling the fiber in a propylene glycol bath heated to 165  $^{\circ}\text{C}$  for about 1 h [12]. The fiber is protected against mechanical stress and breakage, by threading it through a spiral-shaped stainless steel metal hose (i.d.: 4 mm) with a stripwound outer hose (o.d.: 7 mm), before the dissolution process (cf. Fig. 2). Both protection hoses are easily permeable for liquids. After the coating dissolution process, the input end of the fiber was fixed in a ST connector and polished with abrasive paper to minimize coupling losses.

#### 3.2. Mini-OTDR

To demonstrate the feasibility of distributed sensing of HC compounds with long PCS fibers and with an instrument that is applied in real world applications, we have adapted sensing fibers to a portable mini-OTDR (TFS 3031, Tektronix), which is normally used for testing of optical fibers, e.g., in telecommunication networks. The TFS 3031 is a dual-wavelength OTDR capable of performing measurements at wavelengths of 850 and 1300 nm, that can be applied for testing of single- and multimode fibers. The pulse width of the laser diodes can be varied between 10 and 1000 ns. The instrument was combined with different 100  $\mu\text{m}$ -core PCS sensing fibers of up to 934 m length, whose fiber ends were fixed in standard ST connectors. The multimode output port of the instrument is designed for 62.5  $\mu\text{m}$  core fibers typically used in telecommunications. Therefore, laser light launched from the instrument into the 100  $\mu\text{m}$ -core PCS fiber will initially excite only low-order modes in an ‘underfilled fiber’ (launch beam diameter < fiber core diameter). To achieve a stable modal distribution a FM-1 mode scrambler (Newport) was placed at a distance of 30 cm from the input end of



Fig. 3. Photograph of fiber-optical OTDR sensor system for continuous, spatially resolved hydrocarbon leakage control.

the fiber. A photograph of the prototype distributed fiber-optical sensor system for localization of HC leakage is shown in Fig. 3. It consists of the protected sensing fiber that is adapted to the mini-OTDR and a laptop computer for automatic evaluation and documentation of the measurements.

### 3.3. Sample preparation and measurements

The container for measuring the OTDR response to the analyte solutions was a double-walled, thermostated glass jar with an inner diameter of 20 cm and a 2500 ml volume. It was similar to the one described in detail earlier [16]. The fiber section to be contacted with the chemical was led through the lid of the jar and was fixed inside wound up in loops of about 18–20 cm diameter. In most cases a 2 m length of the fiber section has been chosen, but in some experiments the length of the fiber section was varied between 0.75 and 5 m.

After recording the OTDR waveform with the fiber in air or in pure water the analyte solution was poured into the jar and the sample measurement was started. The extraction of an analyte in the fiber cladding was pursued by storing averaged OTDR waveforms at fixed intervals (typically 1–2 min). After the measurement, the liquid HC solution was removed from the sample container and the sensor fiber was regenerated either by evaporating volatile HCs in air or by washing with acetone. The response of the sensing fiber in combination with the mini-OTDR to chemical induced RI changes in the cladding was tested either with pure liquid HCs of different RI and polarity (all of analytical grade quality) or with aqueous HC solutions.



## 4. Results and discussion

### 4.1. OTDR response to cladding RI changes induced by HCs

The penetration of an apolar HC compound into the cladding of a distributed sensing fiber leads to a change in the RI of the matrix surrounding the fiber core. On the one hand, a decrease in the RI of the cladding will occur due to a density reduction associated with swelling of the polymer, and on the other hand, the RI of the extracted HC will contribute to the ‘mixed’ RI of the swollen cladding. Polymer swelling in the presence of analytes will be influenced by the structure of the polymer, e.g., the degree of cross-linkage and the polymer/analyte interaction. An increase in the RI of the cladding for a mode filled fiber strips off higher order modes and decreases the fiber transmittance (cf. Eqs. (8) and (9)).

In Fig. 4 typical OTDR traces are depicted, which were recorded with the distributed sensor system described above. A series of experiments was performed with pure chlorinated HC solvents that were always contacted with 2 m sections of a fiber of 934 m total length. The OTDR reference trace, which was taken with the fiber in air, shows the excitation pulse and the Fresnel reflection from the far end of the fiber, as well as the decrease in the backscatter light level with increasing distance. This decrease depends on the fiber attenuation properties, and from the slope of the trace the loss of the sensing fiber at the 850 nm laser diode wavelength was determined to be  $10.6 \text{ dB km}^{-1}$ . Using this value and the dynamic range of the backscattered light level the maximum length of this fiber for distributed HC sensing was calculated to be in the range of  $\sim 1.0\text{--}1.5 \text{ km}$ . If the fiber is

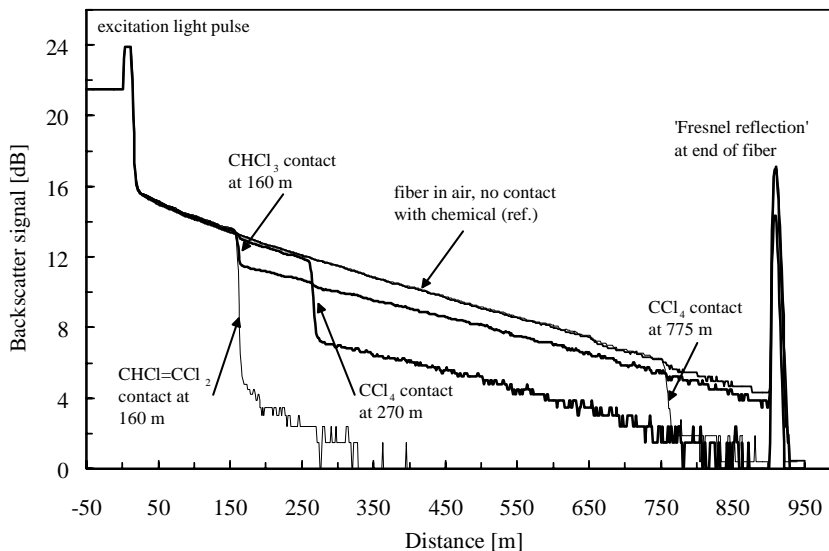


Fig. 4. OTDR traces recorded by distributed fiber-optical sensor system for contact of pure chlorinated hydrocarbons at different positions along the sensing fiber (length of contact zone = 2 m); step drop in backscatter signal intensity indicates position of contact.

immersed in liquid  $\text{CHCl}_3$ ,  $\text{CCl}_4$  or  $\text{CHCl}=\text{CCl}_2$  at different positions along the fiber, discrete ‘step drop’ signals occur at the corresponding section in the OTDR trace, which are an indicator for the position of HC/fiber contact. The step drop in backscatter signal intensity is due to the RI increase in the fiber cladding, which leads to stripping of higher order modes and a corresponding reduced backscatter light level in the fiber beyond this section. The step drop signal height in Fig. 4 increases in the series trichloromethane ( $n_{\text{D}}^{20} = 1.4459$ ) < tetrachloromethane ( $n_{\text{D}}^{20} = 1.4601$ ) < trichloroethene ( $n_{\text{D}}^{20} = 1.4773$ ). The step drop signal caused by trichloromethane extraction is distinct enough for good location of the contact and will also allow identifying further points of contact beyond the first contact zone with the chemical. For trichloroethene on the other hand, the corresponding ‘mixed’ RI in the fiber cladding at the contact zone reaches a value where no light is guided in the fiber beyond the extraction spot and the Fresnel reflection at the fiber end cannot be observed. In this case, it would not be possible to see further contact points beyond this section.

Fig. 4 also depicts two tetrachloromethane traces, where the HC was contacted with fiber sections located at distance of 270 and 775 m from the fiber input end. These traces show that the height of the step drop signal for a modefilled fiber and a given analyte and fiber/analyte interaction length is independent on position along the sensing fiber. The spatial resolution, i.e. the possibility to differentiate between two contact zones is dominated by the laser diode pulse width and ranged in our experiments from 1 to 5 m.

From Eqs. (6)–(9) discussed earlier it can be stated that a step drop signal in the OTDR trace can only be obtained for HCs whose RI exceeds the RI of the cladding ( $n_{\text{D}}^{20} = 1.436$ ). In further experiments with different liquid HC compounds it turned out that besides the RI of the compound also its polarity has an influence on the analyte signal intensity. Due to the hydrophobicity of the silicone cladding only HCs of low polarity will be extracted into the polymer while a polar liquid like water will not penetrate. Table 1 shows RI and polarity data of different liquid HCs and the corresponding step drop signal heights obtained with the distributed fiber-optical sensor system. The  $E_{\text{T}}^{\text{N}}$  values given in Table 1 describe the polarity of a compound on an empirical, spectroscopy based scale given by Reichardt [17]. They are obtained by measuring the shift of the absorbance maximum of solvatochromic dyes dissolved in the corresponding HC solvent. The normalized  $E_{\text{T}}^{\text{N}}$  scale ranges from 0 to 1. The  $E_{\text{T}}^{\text{N}}$  value for tetramethylsilane = 0 marks the boundary of the scale at the low polarity side, while the  $E_{\text{T}}^{\text{N}}$  value for water = 1, stands for the highest polarity. From the data in Table 1 it is obvious, that the height of the step drop signal increases for HC compounds with high RI and low polarity, i.e. with an  $E_{\text{T}}^{\text{N}}$  value close to zero.

In Fig. 5 the normalized step drop signal height data (normalized to the maximum value, i.e. complete light loss at the position of enrichment) are plotted as a function of the quotient of the RI and  $E_{\text{T}}^{\text{N}}$  data of the HC compounds given in Table 1. The experimental data can be fitted by a sigmoidal function (cf. Fig. 5), which in a first approximation allows predicting the signal height of pure liquid HC compounds if their RI and  $E_{\text{T}}^{\text{N}}$  data are known.

#### 4.2. Influence of HC/fiber interaction length on the OTDR response

A distributed chemical sensing system should allow measuring the spatial extension of a fiber segment contacting the chemical. Thus, it is an important aspect whether the

Table 1

Comparison of step drop signal height obtained from pure liquid HCs of varying RI and polarity; step drop signal height = difference signal of analyte and air reference OTDR trace (contact with 2 m fiber section); signals are only obtained for RI > 1.436

Hydrocarbon	Refractive index $n_D^{20}$	$E_T^N$ Reichardt polarity [17]	Step drop signal height (dB)
Dichloromethane	1.4242	0.309	0.02
1,2-Propanediol	1.4324	0.722	0.01
1,2-Dichloroethane	1.4448	0.327	0.33
Trichloromethane	1.4459	0.259	1.46
Acetylacetone	1.4494	0.571	0.15
Cyclohexanone	1.4507	0.281	0.39
1-Methyl-2-pyrrolidone	1.4684	0.355	0.03
1,1,2-Trichloroethane	1.4714	0.296	1.36
Dimethyl sulphoxide	1.477	0.444	0.02
Trichloroethene	1.4773	0.160	8.30
Toluene	1.4961	0.099	8.33
1,3,5-Trimethylbenzene	1.4994	0.068	8.44
Benzene	1.5011	0.111	8.44
Tetrachloroethene	1.5053	0.043	8.52
Pyridine	1.5095	0.302	0.81
Dimethylphtalate	1.5138	0.309	0.01
1,2-Dibromopropane	1.5201	0.259	3.00
Chlorobenzene	1.5241	0.188	8.44
Benzonitrile	1.5289	0.333	0.16
Acetophenone	1.5325	0.306	0.16
Benzyl alcohol	1.5396	0.608	0.02
1,2-Dichlorobenzene	1.5515	0.225	8.43
Aniline	1.5863	0.420	0.10

step drop pattern in the OTDR response function allows extracting additional information on the length of the fiber section that contacts the chemical. Therefore, OTDR measurements with pure trichloromethane were performed, where the length of sensing fiber coming into contact with the hydrocarbon has been increased in discrete steps from 0.75 to 5.0 m.

The inset in Fig. 6 shows two zoomed in OTDR step drop signals obtained during these experiments. From a qualitative comparison of the two signals one can clearly see that both the vertical height and the horizontal width of the step drop increase if the interaction length is extended from 0.75 to 5 m. In Fig. 6 the width and height of the step drop signals caused by trichloromethane extraction have been plotted as a function of the interaction length between sensor fiber and chemical. Here, the width of the step drop signal is defined as the distance between two points directly in front and behind the step drop signal, where the slope of the OTDR trace (attenuation) has the value of the unloaded fiber. Both signals are linearly correlated to the interaction length sensor fiber/chemical. Thus, for a given HC compound or HC mixture in principal one could use both parameters to predict the interaction length. However, due to the fact that the height of the step drop signal additionally is dependent on the RI and polarity of the HC compound, it is preferable to use the width of the step drop in the OTDR response function to calculate the spatial extension of a contact zone.

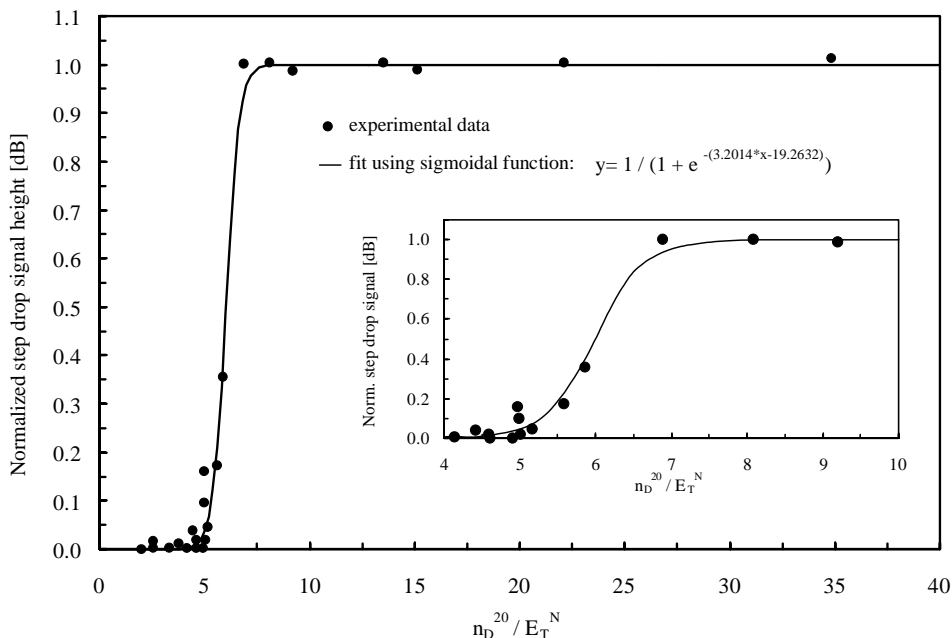


Fig. 5. Normalized step drop signal height plotted as a function of the RI and  $E_T^N$  quotient of the pure HC compounds listed in Table 1; step drop signal height has been normalized to the maximum value (complete light loss).

#### 4.3. OTDR response to cladding RI changes induced by aqueous HC solutions

The hydrophobic silicone cladding of the distributed sensing fiber of the system prevents any interference from water. Thus, it can be applied for the detection of HCs dissolved in water as well. The smaller step drop signals obtained for aqueous solutions of trichloroethene and *p*-xylene resemble those obtained with the pure compounds. Fig. 7 shows the step drop signal height as a function of HC concentration for both HC compounds. For a given HC compound or mixture the vertical height of the step drop signal can be used as a quantitative measure of HC concentration. For both compounds the signal height is linearly correlated with the concentration up to values close to the saturation solubility. The sensitivity of the OTDR measurement for *p*-xylene is by a factor of  $\sim 13$  higher compared with trichloroethene. This is caused by different factors: *p*-xylene ( $E_T^N = 0.074$ , [17]) has a lower polarity and higher RI ( $n_D^{20} = 1.4958$ ) than trichloroethene. Additionally the saturation solubility in water is by a factor of 6 lower, which favors the extraction of the aromatic HC compound in the hydrophobic silicone cladding. The detection limits calculated from the 3-fold standard deviation of the OTDR instrument noise level and the slope of the calibration functions are  $9 \text{ mg l}^{-1}$  for *p*-xylene and  $123 \text{ mg l}^{-1}$  for trichloroethene. The ability of the system to detect apolar HCs in water at these concentrations opens up the possibility for leakage monitoring at liners of waste disposal sites that contain leachable HC compounds.

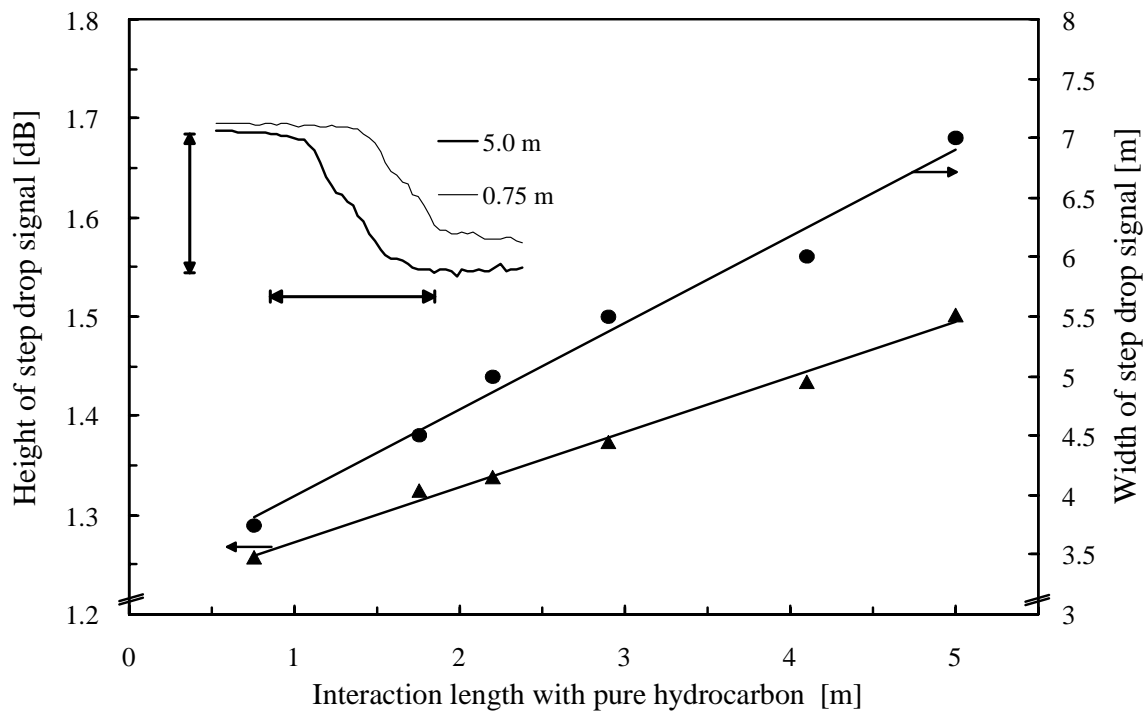


Fig. 6. Dependence of step drop height and width on the interaction length between hydrocarbon and sensing fiber; extraction of pure  $\text{CHCl}_3$ .

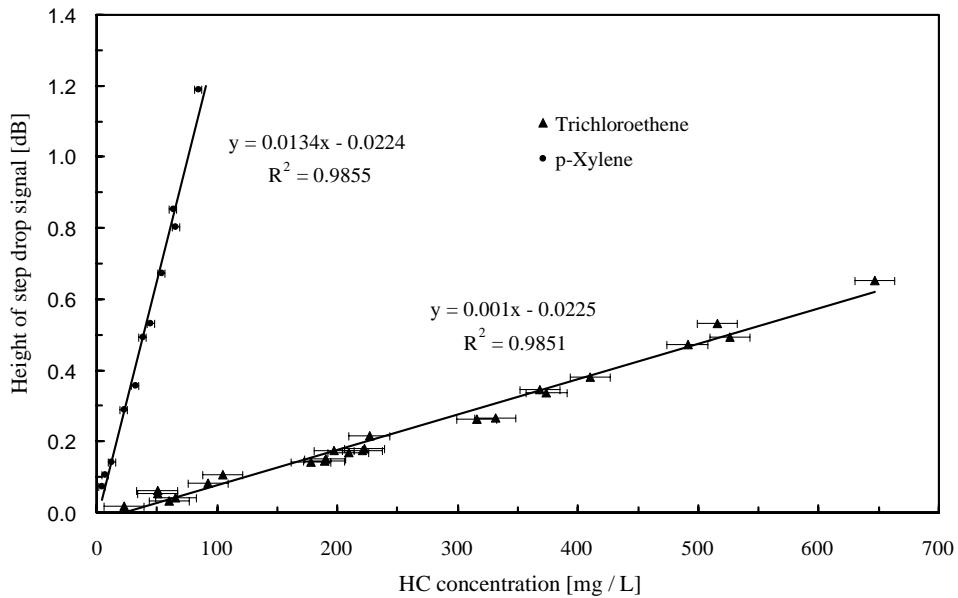


Fig. 7. Step drop signal height vs. HC concentration for aqueous solutions of *p*-xylene and trichloroethene (difference signal of sample solution and water reference); length of contact zone = 2 m.

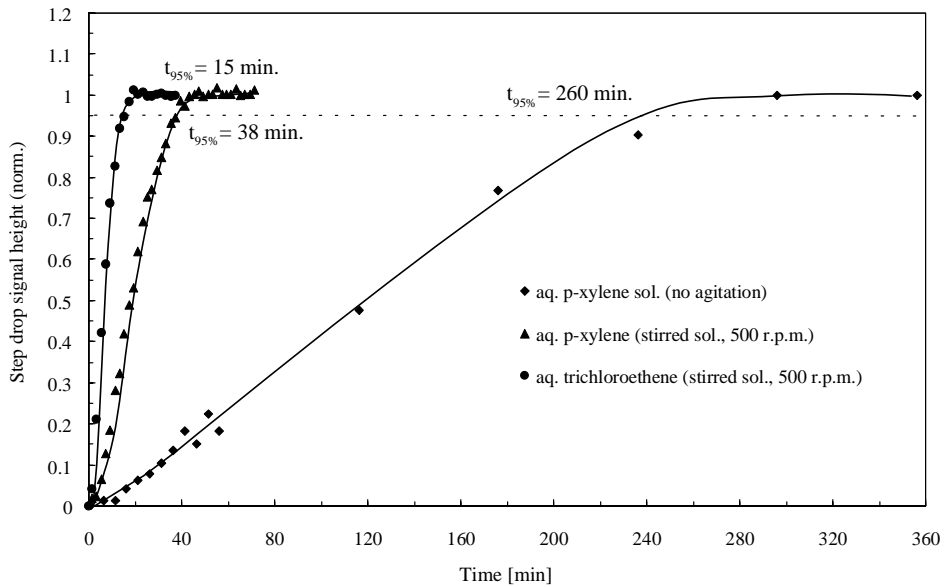


Fig. 8. Response signal vs. time for OTDR-evanescent wave measurements of aqueous *p*-xylene and trichloroethene solutions; length of contact zone = 2 m; response signal: difference step drop signal height of sample solution and water reference normalized to the equilibrium value;  $c_{TCE} = 1016$  mg/l;  $c_{p\text{-xylene}} = 91$  mg/l.

The equilibrium response times of the fiber-optic sensor system for contact with pure liquid HCs are in the range of 3–10 min (usually a first step drop signal can be identified after 30 s). For aqueous solutions on the other hand, the sensor response times for HC compounds strongly depend on the HC species and the hydrodynamic conditions. Typically, diffusion of the HC analyte molecules through the aqueous bulk solution or in case of agitated solutions diffusion through the Prandtl boundary layer at the sensor surface is the rate-determining step [18]. Fig. 8 depicts the response curve of the fiber-optical OTDR system to aqueous solutions of *p*-xylene and trichloroethene. As expected, for both compounds a much longer equilibration time is needed than for the pure compounds. For a stirred aqueous solution, *p*-xylene due to its steric hindrance has a higher  $t_{95\%}$ -value of 38 min (time to reach 95% of the equilibrium signal) than trichloroethene ( $t_{95\%} = 15$  min) [18]. An even longer  $t_{95\%}$ -value of 260 min is obtained for the aromatic HC if the aqueous solution is not stirred. Due to the slow diffusion through the aqueous bulk solution the equilibration time is rather long. However, in applications for landfill or chemical waste disposal containment monitoring, HC leakage due to the slow mobility of groundwater will also be a rather slow process, and thus the response times of the system are compatible with the concentration changes occurring in these environments.

## 5. Conclusions

The investigations presented in this paper prove the feasibility of distributed chemical sensing of liquid apolar HCs and of aqueous HC solutions by using optical time-domain reflectometry in a polymer-clad optical fiber. These features open up possibilities for applications of the distributed fiber-optical sensor system in HC leakage control, e.g. in tank farms or chemical pipelines. Due to the absence of any water interference, the hydrophobic sensor cable can also be deployed in aqueous environments and is able to detect even apolar HCs that are homogeneously dissolved in water. Thus, it could also be applied for leakage monitoring at liners of waste disposal sites. The higher sensitivity could be an advantage compared with commercially available metallic time domain reflectometry (MTDR) systems with HC sensitive coaxial cables.

Further work is in progress to optimize the control software of the sensor system and the evaluation algorithms for automatic location of the position of an HC contact and the spatial extension of a contact zone. Afterwards the system will be tested in the field with real world HC mixtures contained in tanks farms, e.g., gasoline and diesel fuel.

## References

- [1] M.K. Barnoski, S.M. Jensen, *Appl. Opt.* 15 (1976) 2112.
- [2] A.J. Rogers, *Phys. Reports* 169 (1988) 99.
- [3] R.A. Lieberman, in: A.D. Kersey, J.P. Dakin (Eds.), *Distributed and Multiplexed Fiber Optic Sensors*, vol. 1586, SPIE, Bellingham, 1991, pp. 80–91.
- [4] F. Kvasnik, A.D. McGrath, in: R.A. Lieberman, M.T. Włodarczyk (Eds.), *Chemical, Biochemical, and Environmental Fiber Sensors I*, vol. 1172, SPIE, Bellingham, 1989, pp. 75–82.
- [5] C.A. Browne, D.H. Tarrant, M.S. Olteanu, J.W. Mullens, E.L. Chronister, *Anal. Chem.* 68 (1996) 2289.

- [6] R.A. Potyrailo, G.M. Hieftje, *Anal. Chem.* 70 (1998) 1453.
- [7] A. Kharaz, B.E. Jones, *Sens. Actuators A* 46–47 (1995) 491.
- [8] W.C. Michie, B. Culshaw, M. Konstantaki, I. McKenzie, S. Kelly, N.B. Graham, C. Moran, *J. Lightwave Technol.* 13 (1995) 1415.
- [9] W.C. Michie, B. Culshaw, I. McKenzie, M. Konstantaki, N.B. Graham, C. Moran, F. Santos, E. Bergqvist, B. Carlstrom, *Opt. Lett.* 20 (1995) 103.
- [10] J. Bürck, S. Roth, K. Krämer, M. Scholz, N. Klaas, *J. Hazard. Mater.* 83 (2001) 11.
- [11] J. Bürck, E. Sensfelder, in: R.A. Lieberman (Ed.), *Chemical, Biochemical, and Environmental Fiber Sensors X*, vol. 3540, SPIE, Bellingham, 1998, pp. 98–109.
- [12] E. Sensfelder, J. Bürck, H.-J. Ache, *Appl. Spectrosc.* 52 (1998) 1283.
- [13] E.G. Neumann, *Appl. Opt.* 17 (1978) 1675.
- [14] D. Gloge, *Appl. Opt.* 10 (1971) 2252.
- [15] A.W. Snyder, J.D. Love, *Optical Waveguide Theory*, Chapman & Hall, London, 1983, p. 127.
- [16] J. Bürck, E. Sensfelder, H.-J. Ache, in: R.A. Lieberman (Ed.), *Chemical, Biochemical, and Environmental Fiber Sensors IX*, vol. 3105, SPIE, Bellingham, 1997, pp. 21–30.
- [17] Ch. Reichardt, *Chem. Rev.* 94 (1994) 2319.
- [18] J. Bürck, M. Schlagenhof, S. Roth, H. Mathieu, *Field Anal. Chem. Technol.* 5 (2001) 131.